Contribution No. 1475 from the Central Research Department, Experimental Station,
E. I. du Pont de Nemours and Company, Wilmington, Delaware 19898

The Crystal Structure and Transport Properties of $NiRh_2Se_4$

By R. J. BOUCHARD

Received July 17, 1968

A new compound, $NiRh_2Se_4$, has been prepared and found to have the monoclinic defect NiAs structure with space group I2/m and $Z = 2$. Crystal structure analysis was carried out by the powder method; 37 intensities above background were collected by counter methods and refined to an R factor of 5.3%, based on intensities. Rh clusters were found, and the implications regarding metal–metal bonding are discussed. $NiRh_2Se_4$ is compared with the isotypical NiV_2Se_4, where metal–metal interactions cause a contraction in the basal plane of the structure. It is concluded that metal–metal bonding is not important for $NiRh_2Se_4$, although electrical and magnetic properties indicate essentially metallic conduction and Pauli paramagnetism. In addition, a nearly random arrangement of Ni and Rh atoms between the two kinds of available cation sites was found.

Introduction

Compounds of the type AB_2X_4, where A and B are transition metal ions and X is a chalcogen (O, S, Se, Te), are well known. The oxides are all spinels, while the tellurides are nearly all defect NiAs type. The sulfides and selenides can be of either structural type with the incidence of the NiAs-type structure increasing from sulfur to selenium. Within the stability range of the defect NiAs structure, little or no work has been done with second-row transition metals. Rhodium is the most likely element in this series to form a compound of the AB_2X_4 type, since it is the only one which commonly forms oxides where the metal ion is at least formally in the trivalent state, *e.g.*, Rh_2O_3, $LaRhO_3$, and $LiRhO_2$. Moreover, the binary chalcogenides are not so overwhelmingly stable as to preclude the formation of a ternary compound, *viz.*, MoS_2, $RuSe_2$, etc. In addition Rh_2Se_3 is known to exist.[1] Consequently, $NiRh_2Se_4$ was prepared and found to have the monoclinic, ordered defect NiAs structure.[1a] A primary purpose of this investigation was to compare $NiRh_2Se_4$ with the isostructural NiV_2Se_4.

NiV_2Se_4 was shown[2] to have a contraction of the monoclinic unit cell along the a and b directions where direct metal–metal bonding could result from the overlap of t_{2g} wave functions. This "contraction" was relative to $NiCr_2Se_4$, where Cr–Cr interactions were not considered operative along these same directions. A crystal structure determination showed that the vanadium ions had shifted from their "ideal" positions so as to form clusters of vanadium ions with alternating smaller and larger interatomic separations. For comparison, a crystal structure refinement was carried out on $NiRh_2Se_4$. The powder method was used to collect intensity data since experience with monoclinic AB_2X_4 compounds suggests that stoichiometric, single crystals of $NiRh_2Se_4$ would be difficult to obtain, if not impossible.

Experimental Section

$NiRh_2Se_4$ was prepared by heating stoichiometric quantities of the high-purity elements in an evacuated silica tube. The Ni metal was freshly reduced prior to reaction. The tube was heated slowly to 600° until all of the Se had reacted. The sample was then ground under dry N_2, refired to 900° for several days, and cooled slowly over a period of approximately 1 week.

Electrical properties were measured on a sintered bar which was pressed from the finely divided compound at about 30,000 psi, fired to 800° for ~2 days, and cooled slowly to room temperature. A Keithley 150B microvoltammeter was used to measure resistivity by a conventional four-probe method from room temperature to 1000°K.

The magnetic susceptibility was measured by the Faraday method.

For the structure determination, X-rays from a high-intensity copper source were diffracted by the powder, then monochromatized (AMR-202 focusing monochromator), and counted electronically. A Norelco diffractometer and a pulse-height analyzer were used. The diffractometer scanning speed was 0.25° (2θ)/min. Relative intensities were obtained by averaging several fixed-time scans from background to background on either side of each peak. The background under a peak was then subtracted using a curve of background intensity *vs.* angle 2θ. No peak was used unless the net peak to background ratio was greater than 1.0. Lorentz and polarization corrections were applied to these intensities, the polarization factor being the appropriate one for diffraction with a focusing monochromator.

Since all of the reflections could be indexed on the basis of a Cr_3S_4-type defect NiAs structure with ordered vacancies on the nearly hexagonal metal ion sublattice, the ideal structure[3] was used to initiate refinement of the structure of $NiRh_2Se_4$. This trial structure (Figure 1) is based on the monoclinic space group I2/m which is the body-centered equivalent of C2/m. The ideal parameters are given in Table I. The ordering of vacancies (ordered within the plane and confined to every other metal layer) appears to be a prerequisite to the monoclinic AB_2X_4 structure. It is not to be confused with the ordering between the A and B ions to be discussed later.

The program used was SFLS6, an adaptation[4] of the standard Busing, Martin, and Levy least-squares program which was modified to refine intensities (rather than structure factors) and

---

[1] E. Parthe, D. Hohnke, and F. Hulliger, *Acta Cryst.*, **23**, 832 (1967).

[1a] Note Added in Proof.—In a recent publication, R. H. Plovnick and A. Wold, *Inorg. Chem.*, **7**, 2596 (1968), describe the preparation and properties of a number of MRh_2X_4 compounds, among which is $NiRh_2Se_4$. Their electrical data and unit cell parameters are essentially identical with those in this work.

[2] R. J. Bouchard, W. R. Robinson, and A. Wold, *Inorg. Chem.*, **5**, 977 (1966).

[3] F. K. Jellinek, *Acta Cryst.*, **10**, 620 (1957).

[4] C. T. Prewitt, this laboratory, unpublished program.

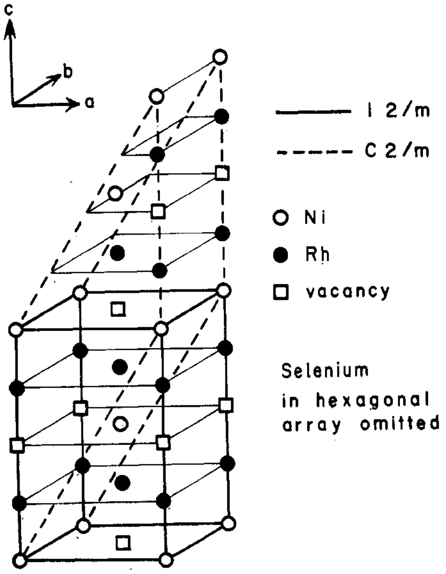

Figure 1.—Ordered defect NiAs structure of $NiRh_2Se_4$ with complete ordering of Ni and Rh atoms.

to allow the use of multiple reflections where two or more reflections occurred so closely spaced in 2θ that they could not be separated for individual counting. The intensities of multiple reflections under one envelope are additive, which, of course, is not true for structure factors.

Throughout the least-squares refinement, intensities (I_c) were calculated using the scattering factors for the neutral atoms with real and imaginary anomalous dispersion corrections[5] applied and the best known atomic positions. The values of six positional parameters, one over-all temperature factor, and one scale factor were adjusted. To obtain the best fit between the observed I_o and the calculated I_c, the value of $R = \Sigma w(I_o - I_c')^2$ was minimized, where w is the weighting factor, $\sqrt{w} = 1/\sigma$, and $\sigma = \sqrt{I_o} + 20$. The intensity $I_c' = \Sigma p I_c$, where p is the multiplicity, and is the sum of the calculated intensities of all of the reflections which could contribute to an observed intensity, as judged by comparing a d-value calculation with the 2θ ranges scanned. In order to augment the number of observations, several multiple peaks were analyzed graphically on a slow-scan diffractometer tracing and separate intensities were assigned to the individual reflections. Where this was done, a σ of twice that value normally assigned by the weighting scheme was assigned. This results in the weights being scaled down by a factor of $^1/_4$ for these reflections. In all, 37 intensities were available as refinement data, of which 19 were peaks corresponding to a single reflection.

Initially, it was assumed in the refinement that the nickel atoms were in the same planes as the vacancies and the Rh atoms were in the filled metal layers (Figure 1). This is reasonable, since neutron diffraction data[6-8] on similar compounds always place the ion which is formally divalent (normally the A ion in the formula AB_2X_4) on these sites. However, using this assumption the R factor would not drop below about 12% and there were several reflections which had very poor agreement between calculated and observed intensities. These reflections, notably 011 and 103, are from planes containing only Ni or only Ni and Se. At this point a mixing parameter was introduced. The fractional occupancy of the Ni in the vacancy planes was varied, and this uniquely determines the Rh in the vacancy planes, and the Ni and Rh in the other planes. This mixing parameter brought the total number of adjusted parameters to 9.

TABLE I

IDEAL STRUCTURE FOR $NiRh_2Se_4$

Space group I2 m/C_{2h}^3; $Z = 2$
(0, 0, 0; $^1/_2$, $^1/_2$, $^1/_2$) +

2 Ni in 2(a): 0, 0, 0
4 Rh in 4(i): $\pm(x, 0, z)$ with $x = 0$, $z = {}^1/_4$
4 Se(I) in 4(i): $\pm(x, 0, z)$ with $x = {}^1/_3$, $z = {}^3/_8$
4 Se(II) in 4(i): $\pm(x, 0, z)$ with $x = {}^1/_3$, $z = {}^7/_8$

Crystallographic Results

To obtain accurate lattice constants, slow-scan diffractometric data were refined by a least-squares program using all of the observed reflections. The following lattice constants resulted for the cell based on the space group I2/m: $a = 6.2821 \pm 0.0007$ Å, $b = 3.6491 \pm 0.0004$ Å, $c = 10.844 \pm 0.001$ Å, $\beta = 92.24 \pm 0.01°$. Every reflection in the X-ray pattern could be indexed on the basis of the above values and the agreement between calculated and observed d values was excellent.

After five cycles of refinement, the R factor based on intensities ($\Sigma|I_o - I_c|/\Sigma I_o$) (see Table II) dropped to 5.3%. The refinement converged, and the shifts in the parameters were much less than the errors in the parameters. The R factor corresponding to only the 19 individual reflections was 6.0%. The final values of the parameters are listed in Table III, and the important bond distances[9] are given in Table IV. The refined value of the amount of Ni in the vacancy planes was 44 ± 5% which gives the following distribution of ions: on A sites: 44% Ni, 56% Rh; on B sites: 28% Ni, 72% Rh. For a completely random arrangement of ions, both sites would have 33% Ni and 66% Rh. The occupancy of the metal sites is therefore slightly enriched (compared to the random arrangement) toward the ideal AB_2X_4 ordering, where only the Ni atoms are in one set of planes and only the Rh atoms are in the others. For that reason and for the sake of simplicity, the tables and diagrams given and the discussion to follow will still refer to Rh–Rh and Ni–Ni separations, etc., as if the atoms were in their ideally ordered positions. It should be understood that both Rh and Ni are really (Rh,Ni), where significant fractions of both Ni and Rh sites are occupied by the other ion. None of the arguments in the discussion is affected by the partial or complete randomizing of the metal ions.

The refined structure can be derived from the ideal structure, as shown in Figure 2, by shifting the atoms half the distances indicated by the arrows. A projection of the atoms located close to the plane $z = {}^1/_4$ is shown

---

(5) "International Tables for X-Ray Crystallography," Vol. III, The Kynoch Press, Birmingham, England, 1962, p 201.

(6) B. Andron and E. F. Bertaut, *J. Phys.* (Paris), **27,** 619 (1966).

(7) B. Andron, G. Berodias, M. Chevreton, and P. Mollard, *Compt. Rend.*, **263,** 621 (1966).

(8) M. Chevreton and B. Andron, *ibid.*, **264,** 316 (1967).

(9) W. R. Busing, K. O. Martin, and H. A. Levy, Report ORNL-TN-305, Oak Ridge National Laboratory, Oak Ridge, Tenn., 1962.

Table II

Calculated and Observed Intensities for $NiRh_2Se_4$

hkl	I_o	I_c	hkl	I_o	I_c	hkl	I_o	I_c
$\bar{1}01$	17,182	16,223	116	4,995	5,353	109	8,097	7,541
002			206	1,618	1,474	503		
101			$\bar{3}05$			$\bar{4}22$		
011	3,837	3,286	$\bar{3}14$			$\bar{5}12$		
$\bar{1}03$	11,524	10,798	$\bar{4}02$	11,443	12,065	$\bar{1}32$		
110			$\bar{2}22$			$\bar{1}27$		
200			$\bar{1}07$			406		
103	3,397	3,033	024			127	3,590	3,241
$\bar{2}02$	3,833	5,485	222			033		
$\bar{1}12$	34,497	34,664	017	703	595	512		
004	27,472	26,823	411	754	1,233	325		
112			$\bar{4}04$	6,074	6,067	$\bar{5}05$	14,657	14,859
202			224			$\bar{3}18$		
013	6,952	7,113	$\bar{1}25$			$\bar{5}14$		
211	3,438	2,304	$\bar{3}21$			$\bar{4}24$		
$\bar{2}04$	8,668	7,500	321	9,421	9,380	$\bar{1}34$		
$\bar{1}14$	21,222	21,446	$\bar{4}13$			134		
114	21,787	21,017	125			$\bar{0}28$		
$\bar{2}13$	14,525	14,094	008			$\bar{2}19$		
204			224			$\bar{2}33$		
$\bar{3}03$	3,028	2,648	404	2,801	3,023	424	10,476	8,986
020	13,575	13,736	$\bar{2}17$	930	912	$\bar{4}17$		
310	23,097	25,081	$\bar{3}23$	1,417	1,541	505		
$\bar{2}06$	2,561	2,340	026	1,540	1,528	318		
$\bar{1}23$	4,073	3,995	217			330	5,273	5,671
116			$\bar{4}06$	587	392	600		
220			$\bar{5}03$	2,344	2,494	$\bar{4}08$		
123			$\bar{2}26$			$\bar{3}27$		
400			226	942	931			
			$\bar{3}25$					

Table III

Final Parameters for $NiRh_2Se_4$[a]

Atom	x	y	z
Ni	0.0	0.0	0.0
Rh	−0.022 (2)	0.0	0.266 (1)
Se(I)	0.347 (3)	0.0	0.366 (2)
Se(II)	0.337 (4)	0.0	0.882 (1)

[a] Numbers in parentheses are $10^3\sigma$, where σ is the standard deviation. Over-all temperature factor, 0.96; scale factor, 0.0186.

Table IV

Interatomic Distances (in Å) for $NiRh_2Se_4$[a]

Rh–Rh, Ni–Ni (along b): 3.6491 (4)
Ni–Rh: 2.89 (1)
Rh–Rh (ab plane): 3.40 (1), 3.90 (2)
Ni–Se(I): 2.50 (1)
Ni–Se(II): 2.52 (2)
Rh–Se(I): 2.52 (2), 2.59 (2)
Rh–Se(II): 2.40 (1), 2.50 (2)
Se(I)–Se(I): 3.30 (2), 3.42 (3), 3.6491 (4)
Se(II)–Se(II): 3.21 (2), 3.53 (2), 3.6491 (4)

Around each Se(I)
2Se–Ni: 2.50 (1)
2Se–Rh: 2.59 (2)
1Se–Rh: 2.52 (2)

Around each Se(II)
2Se–Rh: 2.40 (1)
1Se–Rh: 2.50 (2)
1Se–Ni: 2.52 (2)

[a] Numbers in parentheses are the standard deviations in the last place.

in Figure 3. All of the Rh atoms near this plane would be 3.63 Å apart if the structure were ideal. The refined structure, however, indicates short and long Rh–Rh separations of 3.40 and 3.90 Å, respectively. It should be emphasized therefore that the refined crystal structure shows clusters of rhodium atoms in a pattern exactly analogous to that determined for the vanadium atoms in NiV_2Se_4.[2]

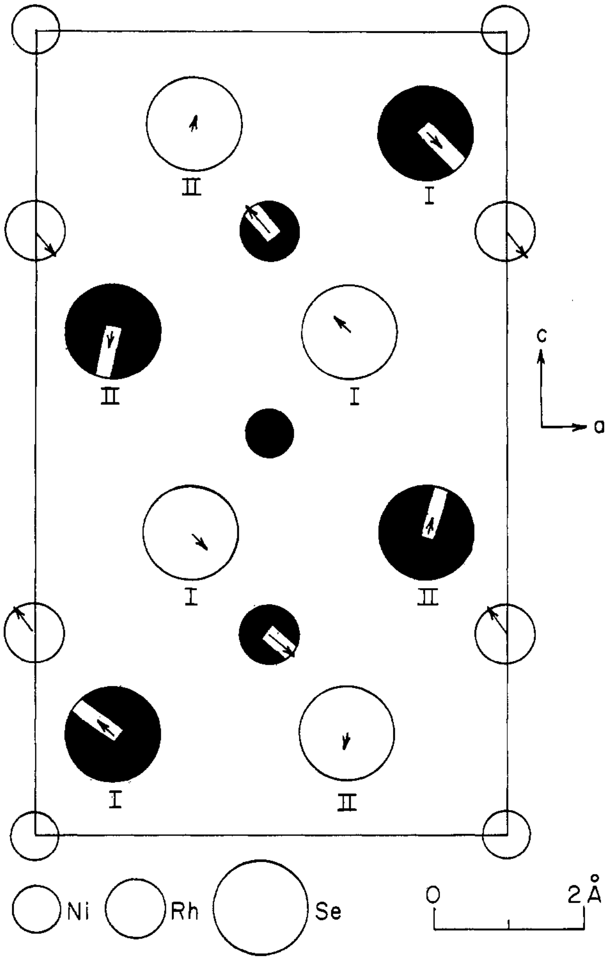

Figure 2.—Trial structure of $NiRh_2Se_4$ and shifts (doubled for emphasis) made in refinement. Dark circles represent atoms at $y = \frac{1}{2}$; open circles represent atoms at $y = 0$. I and II distinguish the crystallographically independent sets of selenium atoms.

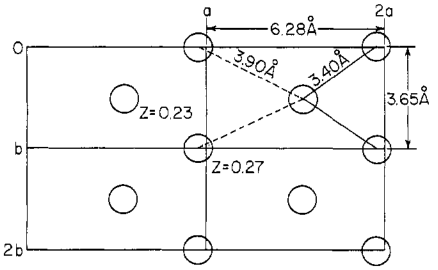

Figure 3.—Rhodium atoms near the plane $z = 1/4$ projected on that plane.

Electrical and Magnetic Properties

The electrical resistivity was 3×10^{-4} ohm-cm at room temperature and remained constant within experimental error to 1000°K. Consistent with this metallic-like behavior, a low Seebeck voltage of $+5$ μV/deg was measured. The magnetic susceptibility was approximately 5×10^{-7} emu/g at 300°K and almost independent of temperature on cooling to about 100°K. The susceptibility gradually increased, however, on further cooling to 4.2°K where $\chi_g = 1.7 \times 10^{-6}$ emu/g. Disregarding the very low-temperature data, the susceptibility is probably best described as Pauli paramagnetic, in agreement with the metallic conductivity observed.

Discussion

Like NiV_2Se_4, the compound $NiRh_2Se_4$ shows metallic conductivity and short metal–metal separations. In an attempt to determine whether the same bonding considerations are important in these seemingly isotypical materials, the NiAs-type structure will be discussed in more detail.

In NiAs, all of the metal atoms are octahedrally coordinated. The octahedra share faces along the *c* axis and edges along the *b* axis and *ab* diagonals. The t_{2g} orbitals of each metal ion are directed to the metal ion nearest neighbors along these directions, meet the symmetry conditions for overlap, and can, at least in principle, form homopolar metal–metal bonds at low temperatures and partially filled band states at some higher temperature. Because the metal ion separations are shortest along the *c* axis (face-sharing octahedra), metal–metal bonding is strongest in this crystallographic direction. When the *defect* NiAs structure is formed, one-fourth of the cations are removed to achieve AB_2X_4 stoichiometry. Since the resulting vacancies are ordered in planes perpendicular to the *c* axis, long-range cooperative metal–metal bonding along this axis is interrupted and weakened. This is especially true for ideal, ordered AB_2X_4 compounds where A atoms see only B atom nearest neighbors in this direction and *vice versa* (Figure 4). Covalent mixing of metal wave functions is less when the metal ions are not identical because of electronegativity differences. The only other possibility for direct metal–metal interactions in AB_2X_4 compounds is in the basal plane where atoms see like neighbors in the same plane (Figure 5). A measure of this interaction is afforded by the *c*/*a* or *c*/*b* axial ratios which will be larger in compounds where metal–metal bonding is strong, reflecting the contraction in the basal plane. It is expected that the bonding will be strongest when the metal ions are at the left of the periodic table, *e.g.*, Ti and V, since the small number of electrons that will occupy the resulting band states will be bonding in nature. In addition, because of the increased orbital extension of the ions at the beginning of the series, bonding will be stronger (for the same internuclear separation) than for the later metal ions of higher nuclear charge. As the number of electrons in the band increases, more antibonding character is imparted until, when the band is full with 6 e^-/transition metal atom, the effective bonding will be reduced to zero. For simplicity a single band is discussed; this assumes that the width of the bonding and antibonding bands is greater than the separation between them. Alternatively, the interaction between any two metal ions could be regarded as the formation of a sixfold degenerate bonding and antibonding band, where the bonding levels would be filled at 3 e^-/transition metal. The next 3 e^-/metal ion would then be antibonding. In this qualitative molecular orbital scheme, the primarily anion-like bonding levels will always be filled and can be ignored for our considerations. The primarily cation-like antibonding d levels will therefore be the last orbitals occupied and we may confine our attention to the d-state manifold. In this case, at least one electron or one hole is necessary in the t_{2g} band for any metal–metal bonding in the system. Very qualitatively, therefore, an inverse relationship is expected between the extent of the metal–metal bonding and the number of t_{2g} electrons per transition metal atom if this kind of bonding is important.

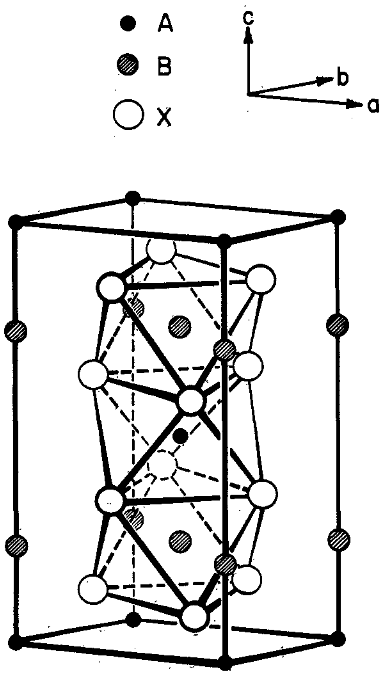

Figure 4.—Face-sharing octahedra along the *c* axis in the ideal, ordered AB_2X_4 defect NiAs structure. Note that A ions see only B ions in this direction and metal–metal interactions are limited to three-atom B–A–B units.

Before examining available experimental data for correlations between the number of d electrons and strength of metal–metal interactions, several assumptions are necessary. First, it is assumed that all of the metal ions are in the low-spin state. This is quite reasonable in compounds where the anion is as polarizable as selenium. In addition, arguments based on critical distance for overlap, which decreases from left to right across the series, are neglected as are the problems associated with the high intraatomic stabili-

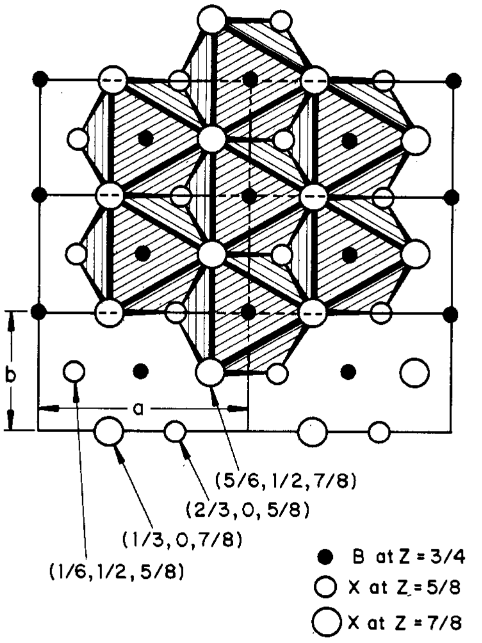

Figure 5.—Edge-sharing octahedra in the basal plane of AB_2X_4 defect NiAs structure. The octahedra as drawn surround the B metal ions in the upper half of the unit cell at $z = {}^1/_4$ The same features are present for the A ion layers, but with alternate strings of b axis octahedra removed.

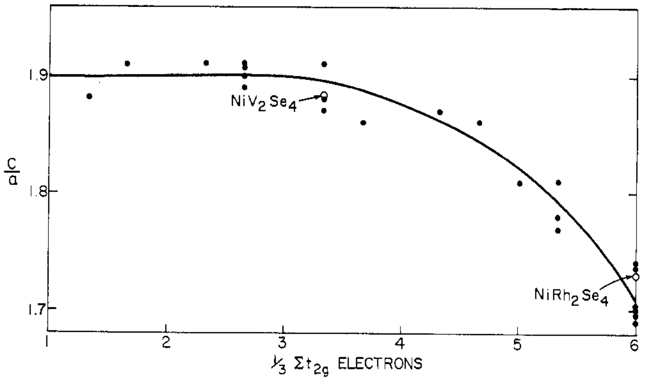

Figure 6.—Variation of c/a with the average number of t_{2g} electrons in AB_2Se_4 compounds.

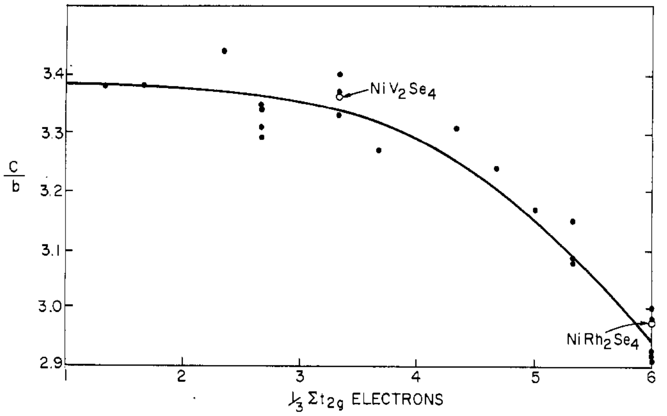

Figure 7.—Variation of c/b with the average number of t_{2g} electrons in AB_2Se_4 compounds.

zation of d^3 ions which will tend to discourage overlap, *e.g.*, between Cr^{3+} ions. In addition, it will be assumed that all metal ions use all of their t_{2g} orbitals for direct overlap with their metal ion nearest neighbors. Even if this is not strictly true, it will not prevent a clear distinction between the case where there is *some* metal–metal bonding and where there is none. To test this model, we used crystallographic data from the work of Berodias, *et al.*,[10] to calculate the c/a and c/b values for a large number of AB_2Se_4 compounds (where A = Ti, V, Cr, Fe, Co,or Ni, and B = Ti, V, Fe, Co, or Ni) and plotted them *vs.* the average number of t_{2g} d electrons per transition metal ion (Figures 6 and 7). Although the values are somewhat scattered, the expected trend in c/a and c/b values is realized, despite the assumptions and simplifications. Note that the c/a and c/b values are almost constant to about 3 e^-/metal ion, after which they decrease rapidly. $NiRh_2Se_4$, as indicated in the figures, clearly is located where little metal–metal bonding is expected, based on the simple model discussed. The c/a and c/b values for NiV_2Se_4, which has a unit cell volume almost identical with that of $NiRh_2Se_4$, are also included for comparison. The disorder between the Ni and Rh atoms does not affect these conclusions, since both have filled t_{2g} levels.

The point to be emphasized is that close metal–metal separations, even in conjunction with metallic conductivity, may or may not indicate metal–metal bonding, depending on various factors. One factor is the number of d electrons in the orbitals responsible for the proposed overlap of the particular metal ions involved. Another is the symmetry of the cation sites, which determines the relative energies and degeneracies of the metal orbitals. The strength of the covalent bonding is important since it largely determines whether the ion will be high or low spin, thereby affecting the number of electrons in low-energy orbitals. For compounds like $NiRh_2Se_4$, completely full cation orbitals should suffer a repulsive potential upon overlap. Actually the movements of the Rh ions may alternatively be viewed as resulting from the repulsive forces encountered by the metal ions sharing octahedral faces along the c axis. If narrow band states could be formed by direct overlap, the electrons would completely fill the band and could not lead to metallic conductivity. One mechanism which could account for the metallic properties in these compounds would involve the broadening of cation levels of e_g symmetry into a band by covalent cation–anion interaction.[11] On this basis, the Ni e_g levels should be half-filled, which could lead to metallic conductivity. This is supported by the lack of a paramagnetic moment on the Ni ion, since

---

(10) G. Berodias and M. Chevreton, *Compt. Rend.*, **261**, 2202 (1965).

(11) J. B. Goodenough, *Bull. Soc. Chim. France*, 1200 (1965).

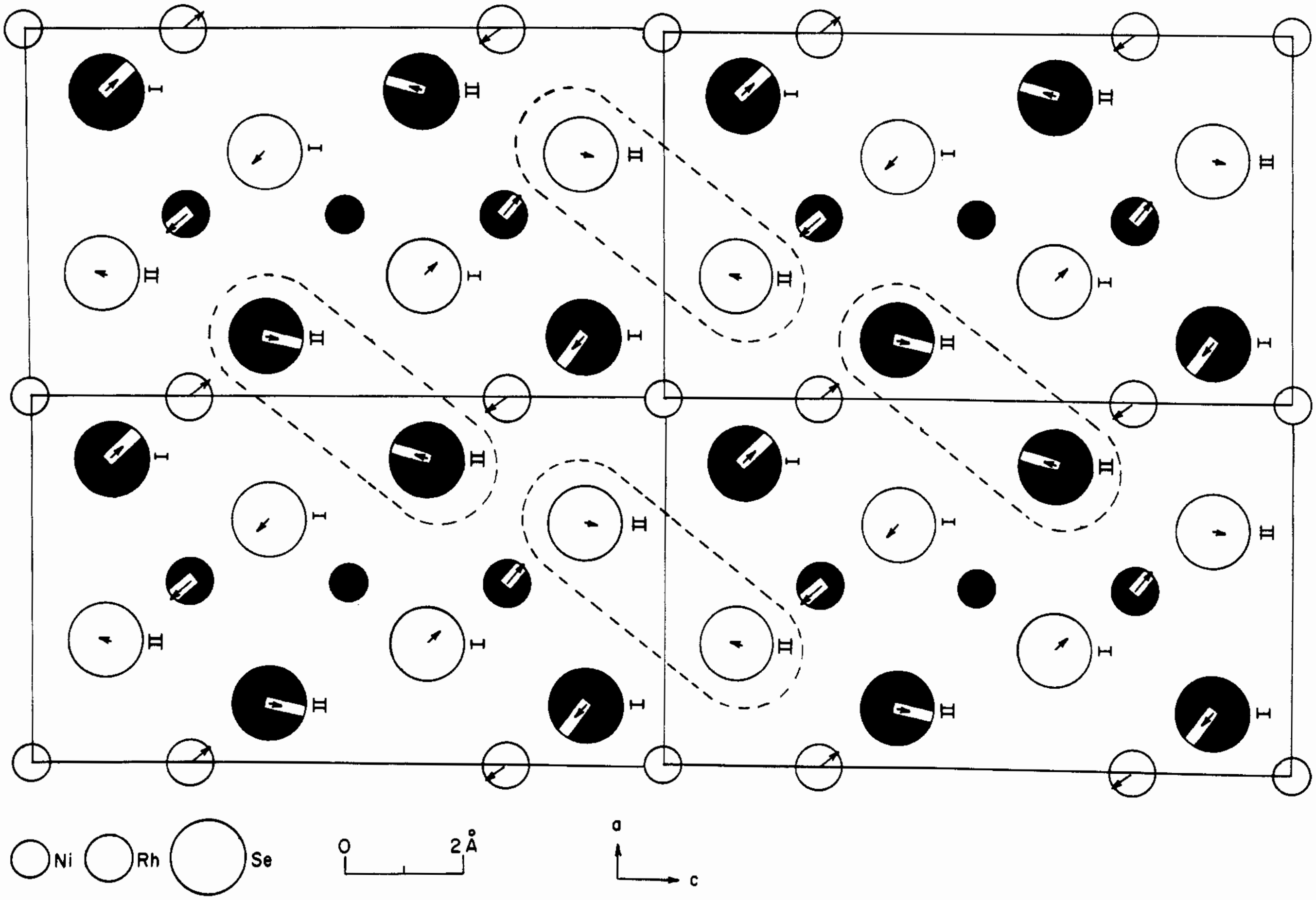

Figure 8.—Four unit cells in the same projection as Figure 2. The formation of Se pairs is indicated by the dashed lines.

low-spin Ni^{2+} on an octahedral site should have a moment corresponding to two unpaired electrons. It may not be possible to attribute the conductivity solely to Ni e_g levels, however, since this assumes that the t_{2g} electrons of the Rh atoms are not involved in any other interaction and that the energy levels associated with them do not overlap any other possible conduction bands in the system. The latter assumption may be somewhat questionable in view of the strong covalent bonding expected between a second-row transition metal and selenium. However, in support of the contention that the conductivity arises from Ni levels, it should be noted that Rh_2Se_3 is semiconducting and diamagnetic.[1]

Finally, it is suggested that the presence of Rh clusters may not be as important as the formation of Se pairs. Figure 8 shows four unit cells in the same projection as Figure 2. It can be seen that all the Se(II) atoms (which are coordinated to only four metal ions) move toward each other. The Se(I) atoms, which are coordinated to five metal atoms, and the metal atoms themselves appear to follow the movements of the Se(II) atoms in an effort to fill the available space more efficiently. The formation of strong anion–anion bonds has been previously observed in the NiAs structure type by Ridgley, *et al.*[12]

Summary and Conclusions

The formation of Rh clusters in $NiRh_2Se_4$ is not attributed to direct metal–metal interaction. In fact, the formation of these clusters occurs when the atoms involved are *either* attracted to each other in the basal plane, as may occur for NiV_2Se_4, *or* repulsed from one another when they share an octahedral face. It appears that the latter effect is about half as important as the former in causing cation displacements, as judged from comparison with NiV_2Se_4 data.[2] It seems doubtful that metal–metal bonding results in any stabilization for the defect NiAs-type phase. Although the fact that the NiAs structure occurs only with transition metal ions has long been attributed to this type of "bonding," it seems more likely that the primary reason is simply the preference for octahedral coordination of transition metal ions in compounds where covalency effects are important. In the NiAs-type structure, all of the metal ions can be octahedrally coordinated, therey placing the largest number of electrons in lower energy orbitals. This tendency is greatly increased for the more polarizable anions because of the large covalent contribution to $10Dq$, the energy splitting between the t_{2g} and e_g orbitals. This is possibly the major reason for the increasing occurrence of the defect NiAs instead of the spinel structure (where the A ions are tetrahedrally coordinated) in the series AB_2O_4, AB_2S_4, AB_2Se_4,

---

[12] D. H. Ridgley and J. H. Geisman, *J. Appl. Phys.*, **39**, 592 (1968).

and AB_2Te_4. The observation that $NiCr_2S_4$ and $NiCr_2Se_4$ are semiconductors, not metals,[13] is another indication that metal–metal bonding is not a prerequisite for the formation of an NiAs-type phase. In addition, the *relatively* small *c*/*a* and *c*/*b* values found in certain AB_2Se_4 compounds suggest that the occurrence of metallic conductivity may best be treated as a phenomenological observation rather than a structural determinant.

Acknowledgments.—The assistance of J. L. Gillson, who measured the resistivity, and J. F. Weiher, who measured the magnetic susceptibility, is gratefully acknowledged. Thanks are given to C. T. Prewitt, who provided the computer program and considerable assistance in its use. A. W. Sleight is thanked for his help in this respect. Discussions with D. B. Rogers are also appreciated.

[13] R. J. Bouchard and A. Wold, *J. Phys. Chem. Solids*, **27**, 591 (1966).

CONTRIBUTION FROM THE LAWRENCE RADIATION LABORATORY AND DEPARTMENT OF CHEMISTRY,
UNIVERSITY OF CALIFORNIA, BERKELEY, CALIFORNIA 94720, AND DEPARTMENT OF CHEMISTRY,
PRINCETON UNIVERSITY, PRINCETON, NEW JERSEY 08540

The Crystal Structure of a Hexanuclear Basic Lead(II) Perchlorate Hydrate: $Pb_6O(OH)_6(ClO_4)_4 \cdot H_2O$[1a]

BY THOMAS G. SPIRO[1b], DAVID H. TEMPLETON,[1c] AND ALLAN ZALKIN[1c]

Received April 26, 1968

The structure of $Pb_6O(OH)_6(ClO_4)_4 \cdot H_2O$ has been determined by single-crystal X-ray diffraction. The crystals are orthorhombic, space group Pbca, $Z = 8$, $a = 10.814 \pm 0.005$ Å, $b = 16.706 \pm 0.006$ Å, $c = 26.273 \pm 0.008$ Å, $d_x = 4.973$ g/cm³, $d_m = 5.07 \pm 0.03$ g/cm³. The structure was refined to a conventional *R* factor of 5.5%, using 791 intensities which were collected by counter methods. The crystal contains discrete $Pb_6O(OH)_6^{4+}$ units. Four of the lead atoms are found in a central tetrahedron (distorted) while the remaining two cover two of the tetrahedral faces, thereby forming two exterior tetrahedra. The adjacent Pb–Pb distances average 3.81 Å and range from 3.44 to 4.09 Å. A unique oxygen atom (oxide) is found at the center of the central lead tetrahedron. The remaining six oxygen atoms, presumably hydroxide, are located over the six external faces of the two exterior lead tetrahedra. These results contradict an earlier conclusion from Raman evidence that the lead atoms are at the corners of an octahedron.

Introduction

Recently Maroni and Spiro[2] investigated the vibrational spectra of a series of hydroxy- and alkoxy-bridged polyhedra of Bi(III), Pb(II), and Tl(I). The most significant result was the finding of a set of low-frequency Raman bands attributable almost entirely to the motions of the metal atoms. The high intensity of these bands was taken as evidence for some degree of metal–metal bonding and the simplicity of their pattern suggested that they might be useful in structural characterization of polynuclear species.

Of particular interest in the latter connection were the species present in perchlorate solutions of lead(II) containing 1.33 mol of hydroxide per mole of lead. Potentiometric[3] and ultracentrifuge[4] data were consistent with an equilibrium between $Pb_3(OH)_4^{2+}$ and $Pb_6(OH)_8^{4+}$. Crystals of composition $Pb_3(OH)_4(ClO_4)_2$ were described in 1930 by Willard and Kassner.[5] The Raman spectrum[2b] of these crystals showed three strong low-frequency bands similar to those exhibited[2a] by octahedral $Bi_6(OH)_{12}^{6+}$. Since in the concentrated solutions from which the crystals were obtained $Pb_6(OH)_8^{4+}$ was presumably predominant, it was inferred that these crystals also contained this complex, and its structure was predicted to be octahedral.[2b] The eight hydroxide ions were presumed to lie above the eight trigonal faces of the lead octahedron, giving a structure analogous to that of $Mo_6Cl_8^{4+}$.[6] A normal-coordinate analysis[2b] showed that this structure was capable of predicting all of the observed Raman and infrared bands of the crystals.

We report here a determination of the structure of these crystals by X-ray diffraction. The results are consistent with the chemical analysis by Willard and Kassner[5] but indicate that the crystals should be formulated as $Pb_6O(OH)_6(ClO_4)_4 \cdot H_2O$ and that the

---

[1] (a) Work done under auspices of the Atomic Energy Commission. Supported in part by Public Health Service Research Grant GM13498 to T. G. S. (b) Princeton University. (c) University of California.

[2] V. A. Maroni and T. G. Spiro, *Inorg. Chem.*: (a) **7**, 183 (1968); (b) **7**, 188 (1968); (c) **7**, 193 (1968).

[3] A. Olin, *Acta Chem. Scand.*, **14**, 126, 814, 1999 (1960); *Svensk Kem. Tidskr.*, **73**, 482 (1961).

[4] O. E. Esval and J. S. Johnson, *J. Phys. Chem.*, **69**, 959 (1965).

[5] H. H. Willard and J. L. Kassner, *J. Am. Chem. Soc.*, **52**, 2395 (1930).

[6] C. Brosset, *Arkiv Kemi*, **1**, 353 (1949); *Arkiv Kemi, Mineral. Geol.*, **A20**, No. 7 (1945).